

Radar Altimetry as a Robust Tool for Monitoring the Active Lava Lake at Erebus Volcano, Antarctica

N. J. Peters¹, C. Oppenheimer¹, P. Brennan², L. B. Lok², M. Ash³, P. Kyle⁴

¹Department of Geography, University of Cambridge, Downing Place, Cambridge, CB2 3EN, UK

²Department of Electronic & Electrical Engineering, University College London, Torrington Place, London, WC1E 7JE, UK

³PA Consulting Group, Global Innovation and Technology Centre, Back Lane, Melbourn, Herts, SG8 6DP, UK

⁴Department of Earth and Environmental Sciences, New Mexico Institute of Mining and Technology, Socorro, NM 87801, USA

Key Points:

- The level of active lava lakes is a key parameter in their study but surprisingly hard to measure
- Eredar is a new radar system for monitoring surface level of active lava lakes
- At Erebus volcano it collected the longest time series of lake level to date

Corresponding author: Nial Peters, njp39@cam.ac.uk

Abstract

The level of lava within a volcanic conduit reflects the overpressure within a connected magma reservoir. Continuous monitoring of lava level can therefore provide critical insights into volcanic processes, and aid hazard assessment. However, accurate measurements of lava level are not easy to make, partly owing to the often dense fumes that hinder optical techniques. Here, we present the first radar instrument designed for the purpose of monitoring lava level, and report on its successful operation at Erebus volcano, Antarctica. We describe the hardware and data processing steps followed to extract a time series of lava lake level, demonstrating that we can readily resolve ~ 1 m cyclic variations in lake level that have previously been recognised at Erebus volcano. The performance of the radar (continuous, automated data collection in temperatures of around -30°C) indicates the suitability of this approach for sustained automated measurements at Erebus and other volcanoes with lava lakes.

1 Plain Language Summary

Active lava lakes are the exposed top of a volcano's magmatic plumbing system. Although only found at a handful of volcanoes worldwide, they are important because they allow direct measurements of magmatic processes which at other volcanoes occur underground and out of sight. The surface level of these lakes is an important parameter to monitor because it reflects pressure changes in the underlying magmatic system. However, it is remarkably difficult to measure because their surface is often obscured by the volcanic gases emanating from the lava. We have developed the first radar instrument for monitoring lava lake level, which can effectively "see through" the volcanic gases, providing an accurate measure of lake level regardless of visibility. The radar was deployed at Erebus volcano, Antarctica and successfully recorded the longest duration measurements of its lava lake's surface level made to date. The radar was able to clearly resolve the metre-scale variations in lake level that have previously been documented at Erebus. Our study shows that radar is an excellent solution for long-duration studies of lava lakes and we are working on refining our design into an operational tool to support volcanological studies and hazard assessment at other volcanoes around the world.

2 Introduction

Open-vent volcanoes maintain magma at or close to the surface, with persistent outputs of heat and gases [Rose *et al.*, 2013]. At the majority of these volcanoes, the interface between the magma and the atmosphere is obscured or only intermittently exposed within a narrow vent. However, a handful of open-vent volcanoes expose magma in plain view from the crater rim, in the form of an active lava lake which may persist for many decades [Tazieff, 1994]. Examples are found at Nyiragongo (D.R. Congo), Erebus (Antarctica) and Erta 'Ale (Ethiopia). Such volcanoes are of particular importance to volcanology as they allow direct observations to be made of magmatic processes that are normally hidden from view. Studies of active lava lakes have revealed many aspects of magma storage, transport, degassing and eruption, highlighting also processes occurring within magma storage zones, conduit and the lake itself [Patrick *et al.*, 2016].

A key parameter in studying lava lakes, is their surface level. This is indicative of pressure variations in the underlying magmatic system [Patrick *et al.*, 2014], and also fluctuates (typically on shorter time scales) in response to shallower processes such as gas accumulation/release from the lake [Orr and Rea, 2012], and flow dynamics in the conduit [Peters *et al.*, 2014a; Jones *et al.*, 2015].

Perhaps somewhat surprisingly, the surface level of active lava lakes is remarkably difficult to measure, especially over the extended time periods required for understanding their behaviour and for operational monitoring. Previous studies [e.g. Patrick *et al.*,

2014] have used thermal camera images, identifying the position of the surface against the back wall of the lake basin (either manually, or using an automated approach) to estimate the surface height. However, the high temperature maintained by the encompassing basin following a rapid draining of the lake makes the margin difficult to identify for an automated system, and manual identification is extremely time consuming. Furthermore, this approach is affected by changes in the basin geometry and cannot detect level changes due to uplift or subsidence of the crater itself. It should also be noted that even at thermal infrared wavelengths, visibility of the lake can be, and particularly at Erebus often is, severely impacted by the volcanic plume. Plume opacity also impedes the use of stereo-imaging systems [Smets *et al.*, 2017] and terrestrial laser scanning (TLS) technologies. TLS is a widely used tool in geoscience [Telling *et al.*, 2017] and although some lava lake studies have been conducted using such devices [e.g., Jones *et al.*, 2015] they are limited to rare time periods of exceptional visibility. TLS instruments are also expensive and delicate making them unsuitable for long-duration deployment at volcanic craters.

Here we demonstrate that radar is an effective solution to lava lake level monitoring. Using a low cost, custom built radar system, named Eredar, we were able to obtain the longest continuous measurements of lake level at Erebus volcano to date, easily resolving the ~ 0.5 m variations in level that are typical of its behaviour [Peters *et al.*, 2014a; Jones *et al.*, 2015].

The aims of this article are twofold: (i) To present the design of our radar system and our data processing strategy, which we believe will be of use to researchers undertaking radar system development in other fields, not just volcanology. (ii) To demonstrate the potential of radar for continuous and extended (operational) lava lake surveillance.

3 Erebus Volcano

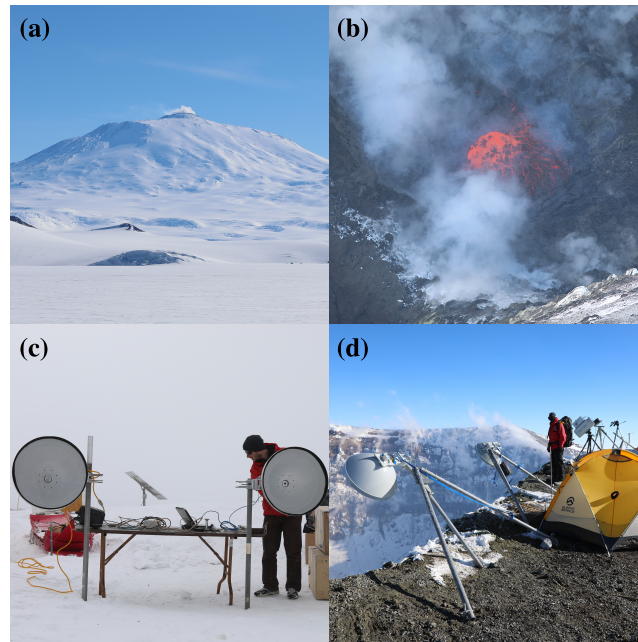
Situated on Ross Island, Antarctica, Erebus is a 3794-m-high active stratovolcano (Fig. 1a). It is the world's most southerly active volcano, and hosts the only known example of a phonolitic active lava lake (Fig. 1b) [Kelly *et al.*, 2008]. The lake at Erebus has been in place since at least 1972 [Giggenbach *et al.*, 1973], and is characterised by stable convective behaviour punctuated sporadically by Strombolian-type explosions caused by gas slugs entering the lake. Some of these explosions are large enough to partially empty the lake, with ejected material occasionally being thrown clear of the crater [Dibble *et al.*, 2008; Jones *et al.*, 2008]. During periods of quiescence the lake exhibits a remarkable pulsatory behaviour [Oppenheimer *et al.*, 2009], with its surface motion, surface level, gas composition and gas flux all varying on a timescale of 10-15 mins [Peters *et al.*, 2014a]. This behaviour is thought to reflect the flow dynamics of magma in the conduit feeding the lake [Oppenheimer *et al.*, 2009; Peters *et al.*, 2014b], however, a comprehensive explanation has proved elusive and provides, in part, the motivation for the development of the Eredar radar system.

The Erebus lava lake was the subject of a previous study using radar undertaken by Gerst *et al.* [2013]. However, this study focused on analysing the evolution of explosive events in the lake, using a Doppler radar system to measure the expansion rate of large bubbles at the surface. No attempt to monitor the surface level of the lake was made, and the radar system was not considered for long-term deployment.

4 Methods

4.1 Field Deployment

Fieldwork on Erebus is conducted during the Austral Summer, typically between late November and early January. The Eredar radar was deployed on Erebus as part of



109 **Figure 1.** Field deployment of the Eredar radar in December 2016; (a) Erebus volcano, (b) its
 110 active lava lake as it appeared in 2016 (~ 30 m in diameter), (c) Eredar being tested at the field
 111 camp, (d) Eredar installed at the crater rim. The radar electronics are housed in the black case
 112 mounted on the far antenna tripod. The thermal camera and other monitoring instruments can
 113 be seen in the background.

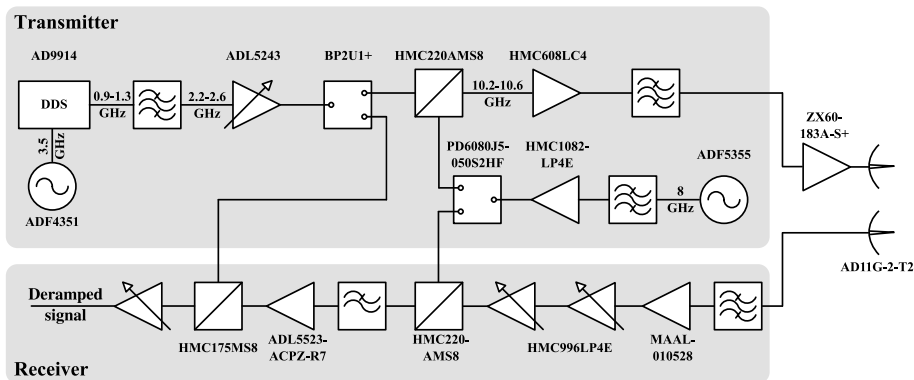
118 the Mount Erebus Volcano Observatory’s (MEVO) 2016 field campaign. Its installation
 119 was hampered by bad weather and it was not in-place until the very end of the campaign,
 120 resulting in a relatively short dataset being obtained.

121 After initial testing at our field camp at around 3450 m elevation (Fig. 1c), The
 122 radar was installed at the so-called “Shackleton’s Cairn” site on the northern side of the
 123 main crater, alongside MEVO’s thermal camera (Fig. 1d) [Peters *et al.*, 2014c]. The an-
 124 tennas were mounted on custom-built heavy duty tripods, which were securely anchored
 125 to the ground. A tent was erected nearby to house the data-acquisition laptop and to
 126 provide shelter for the operator during the setup process. Alignment of the antennas with
 127 the lava lake was achieved by placing an infrared thermometer into their waveguide feeds.
 128 The thermometer had approximately the same field of view as the antenna beamwidth,
 129 and the antennas could then be pointed at the lake by adjusting them until a maximum
 130 temperature was recorded. The thermometer was removed prior to making radar mea-
 131 surements.

132 Following a supervised period of operation lasting ~ 6 hours on 15 December 2016,
 133 the radar was taken down again to avoid damage from an approaching storm. It was then
 134 redeployed on 19 December 2016 and ran, without user intervention, until it had to be
 135 shut-down and removed at the end of the field season (21 hours later). The ambient tem-
 136 perature at the crater rim during this period was approximately -30°C .

137 4.2 Radar Hardware

138 The Eredar instrument is a bespoke, Frequency Modulated Continuous Wave (FMCW)
 139 radar [e.g., Griffiths, 1990; Marshall and Koh, 2008] operating at X-band (10.2-10.6 GHz).



146 **Figure 2.** Simplified block diagram of the Eredar radar system. Some blocks represent an
 147 aggregation of several components and therefore do not have part numbers.

140 Its design is loosely based on two previous geoscience radars constructed by researchers
 141 at University College London, namely the Auto-pRES instrument (UHF, 300 MHz) used
 142 for ice-shelf sounding [Lok *et al.*, 2015] and the Geodar2 system (C-band, 5.3 GHz) used
 143 for avalanche monitoring [Ash *et al.*, 2014]. Due to the requirement of a narrow beamwidth
 144 for lava lake monitoring, the Eredar system operates at much higher frequency than these
 145 previous systems and therefore the details of its design are unique.

148 Figure 2 shows a overview of the Eredar design. An Analog Devices AD9914 Di-
 149 rect Digital Synthesiser (DDS) clocked at 3.5 GHz is used to produce a 900-1300 MHz
 150 linear sweep in frequency. A bandpass filter is then used to select the first super-Nyquist
 151 image [e.g. Ash and Brennan, 2015] of this sweep at 2.6-2.2 GHz. The signal is ampli-
 152 fied, split to provide the deramp signal for the receive chain, and then up-converted us-
 153 ing an 8 GHz source produced by an Analog Devices ADF5355 synthesiser. A bandpass
 154 filter is used to remove unwanted mixing products resulting in a transmitted chirp (lin-
 155 ear frequency sweep) of 10.6-10.2 GHz. A chirp duration of 0.16 seconds was used. To
 156 overcome higher than expected losses in our transmitter chain we included an additional
 157 amplifier between the transmit output and the antenna. This brought our transmitted
 158 power up to ~ 15 dBm. On the receive side, the incoming signal is filtered and ampli-
 159 fied using a chain of three low noise amplifiers, before being down-converted using the
 160 8 GHz signal and subsequently using the deramp signal from the transmitter. The de-
 161 ramped signal is then passed through an active filter stage which performs frequency-
 162 gain control [Stove, 1992, 2004] to compensate for the drop in signal strength with range,
 163 thus maximising the dynamic range available from the system’s analogue to digital con-
 164 verter (ADC). Additionally, the active filter suppresses signals above the Nyquist fre-
 165 quency of the ADC (>40 kHz) and also removes low frequency signals caused by direct
 166 coupling between transmitter and receiver. The filtered, deramped signal is digitised us-
 167 ing a 16 bit ADC clocked at 80 kHz. The ADC clock is precisely aligned with the control
 168 signal to the DDS used to initiate frequency ramping, ensuring inter-chirp coher-
 169 ence in a similar manner to Brennan *et al.* [2014]. Eredar’s on-board microprocessor is
 170 not sufficiently powerful to perform realtime processing on the digitised data. Instead,
 171 it is streamed over Ethernet and recorded on a laptop computer, with all processing be-
 172 ing performed “off-line” at a later date. Ten chirps were averaged for each measurement
 173 and measurements were made at a rate of ~ 0.25 Hz.

174 Both transmit and receive use 66 cm diameter Trango AD11G-2-T2 dish antennas,
 175 with a 3 dB beamwidth of 3.6 degrees and a gain of 36 dBi. Given a range of 315 m and
 176 an incidence angle of 43 degrees (typical viewing geometry of the lake at Erebus; Fig 1d)

177 this gives a beam footprint approximately 27 m in diameter at the surface of the lake.
 178 This is comparable to the lake size itself, which typically varies between 30-50 m in di-
 179 ameter (Fig 1b).

180 The crater rim of Erebus is provided with 230 V AC power from a nearby solar and
 181 wind generation site (see *Peters et al.* [2014c] for details). Due to its requirement of both
 182 positive and negative voltage supplies, the radar uses a centre-tapped transformer and
 183 diode network to step-down and rectify the mains supply producing +7 VDC and -7 VDC.
 184 These supplies are then fed into a bank of linear regulators to produce the various sup-
 185 ply rails required. Switching power supplies were deliberately avoided to keep noise on
 186 the power rails to a minimum. Total power consumption is in the order of 21 W, although
 187 around 50 % of this is dissipated as heat in the linear regulators.

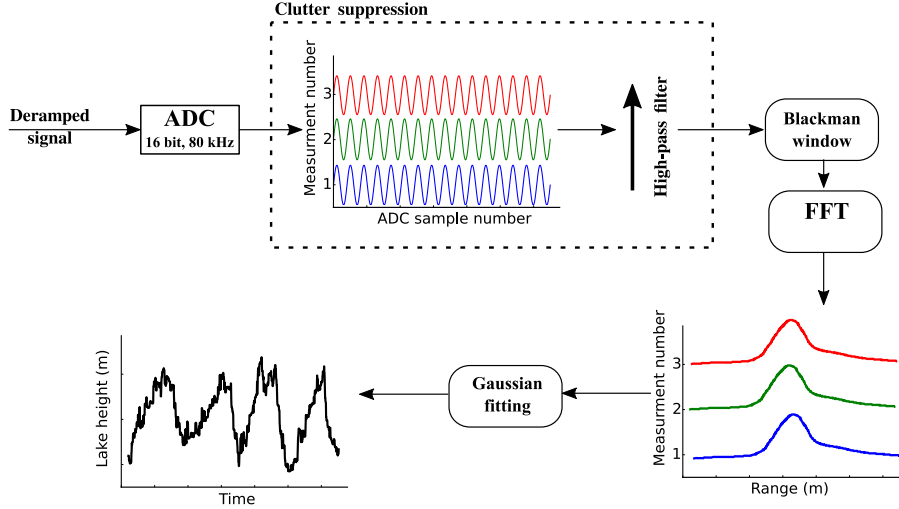
188 The 10.2-10.6 GHz frequency range was selected as a compromise between the cost
 189 of components and the requirement of a narrow beamwidth. For a given antenna size,
 190 beamwidth scales inversely with frequency. However, above 11 GHz there are very few
 191 mass produced components available, resulting in a considerable increase in price.

192 **4.3 Data Processing**

193 The data processing steps required to obtain a lake level measurement from the re-
 194 ceiver output are shown in Fig. 3. The data are first conditioned using a clutter suppres-
 195 sion algorithm (described below) to remove stationary targets. They are then windowed
 196 using a Blackman window and Fourier Transformed using an FFT algorithm. The Black-
 197 man window is used to remove edge discontinuities that would otherwise be caused by
 198 the implicit rectangular window imposed by the finite duration of sampling. The win-
 199 dowed data is zero-padded up to a length of 2^{16} prior to applying the FFT. Range is ob-
 200 tained from the frequency (post-FFT) data using the standard FMCW range equation
 201 [e.g. *Griffiths*, 1990] $r = f \cdot \frac{c\tau}{2B}$ where r is range, f is frequency, c is the propagation
 202 velocity, τ is the chirp period and B is the chirp bandwidth. This assumes that objects
 203 are not moving during the chirp period, a reasonable assumption at Erebus where typ-
 204 ical lake surface velocities are in the order of cm s^{-1} [*Peters et al.*, 2014b]. The lake level
 205 is extracted from the range data by applying a Gaussian fit to it, as described below.

213 **4.3.1 Clutter Suppression**

214 Clutter (unwanted targets within a radar’s field of view) is a common problem for
 215 surface viewing radars and many approaches have been developed to suppress it [e.g. *Mar-*
 216 *tone et al.*, 2014; *Hyun et al.*, 2016; *Ash et al.*, 2018]. The crater in which the Erebus
 217 lava lake resides is littered with lava bombs and angular rocks from the crater walls. These
 218 have a much larger radar cross-section compared to the relatively flat surface of the lava
 219 lake and produce strong reflections even when not at boresight. The clutter signal was
 220 found to be so great, that the much weaker lake signal was entirely masked. A common
 221 approach to recovering a moving target signal from a stationary-clutter dominated mea-
 222 surement is to high-pass filter the range-time data to remove stationary targets. Although
 223 this approach was found to work well when recovering point targets (e.g. a person walk-
 224 ing in the radar beam) during testing, it did not work with data collected of the lake.
 225 This was partly due to the low velocity of the lake surface parallel to boresight (on the
 226 order of $1 \times 10^{-3} \text{ m s}^{-1}$), and partly due to the lake being a distributed target. The radar’s
 227 oblique view of the lake means that its surface occupies many range bins in the recorded
 228 data. A change in surface level of the lake manifests itself as a rather subtle change in
 229 the distribution of amplitudes across these range bins, and as such is severely muted by
 230 high-pass filtering. Instead, we adopted a similar approach to *Ash et al.* [2018], perform-
 231 ing clutter suppression on the raw radar data prior to conversion to range. Chirps from
 232 a measurement period are stacked coherently in time, and then high-pass filtered before
 233 being Fourier Transformed and converted to range. Such an approach is made possible



206 **Figure 3.** Block diagram showing the data processing steps required to go from raw receiver
 207 output to lake level measurements. Each chirp is digitised and recorded. The digitised data are
 208 then high-pass filtered across all measurements to remove static clutter. Filtered data are then
 209 Blackman windowed and Fourier Transformed to convert to range. The lake is identified in the
 210 range data by fitting a Gaussian to it. The mean of this Gaussian is used as the slant-range
 211 to the lake. Finally, the slant-ranges may be easily converted to lake level by considering the
 212 viewing geometry.

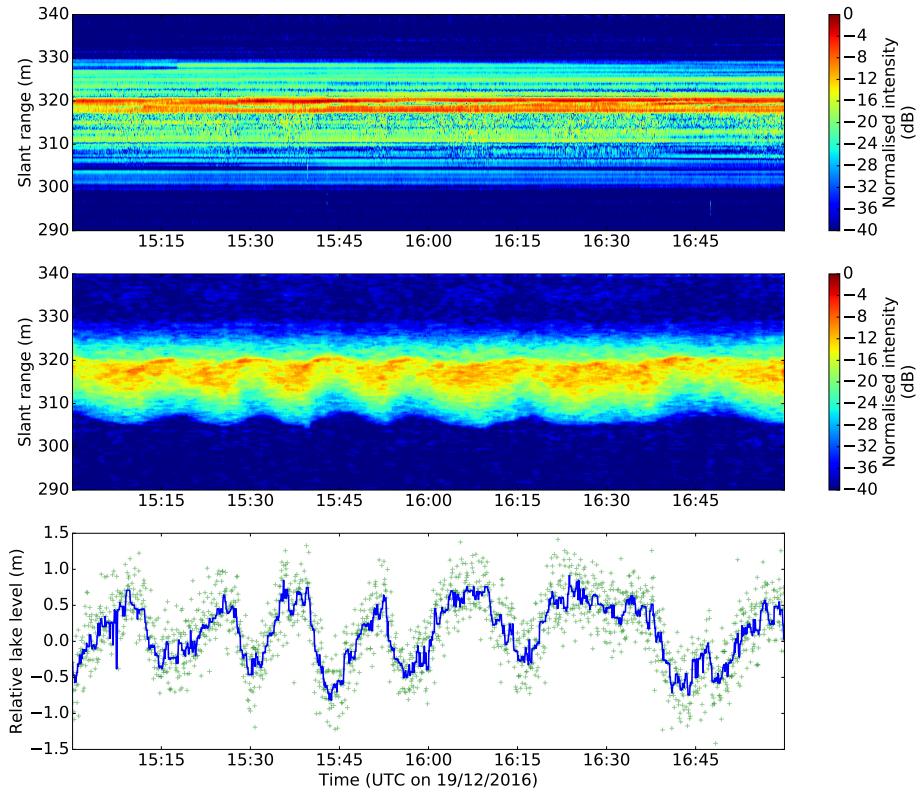
234 by the high degree of coherence between chirps of the Eredar system. We used an in-
 235 finite impulse response (IIR) high-pass elliptic filter with an order of 10 and a cut-off fre-
 236 quency of 3×10^{-2} Hz.

237 4.3.2 Lake Level Calculation

238 As noted above, the lake surface spans many range bins and as such manifests it-
 239 self as a broad, smeared-out return rather than a sharp peak in range. Assuming an ap-
 240 proximately uniform cross-section for all parts of the lake surface, the shape of this re-
 241 turn is dominated by the radiation pattern of the antennas (note that the drop in re-
 242 turn power due to increasing range is already accounted for by the active filter stage in
 243 the radar hardware). To a good approximation, the antenna radiation pattern can be
 244 modelled as a Gaussian. Therefore, to determine the lake level we fitted a Gaussian func-
 245 tion to each measurement, and used the mean of the fitted function as the slant-range
 246 to the lake. The slant-range was then converted to a relative lake level using the follow-
 247 ing equation $L = (\bar{r} - r) \sin \theta$ where L is relative lake level, \bar{r} is mean slant-range (de-
 248 termined from the full time series of measurements), r is slant-range and θ is the graz-
 249 ing angle of the radar beam on the lake surface (measured as 42° using an inclinome-
 250 ter). Thus, a low-stand of the lake (resulting in a higher than average slant-range) gives
 251 a negative value of relative lake level.

252 5 Results and Discussion

253 Figure 4 shows a representative 2 hour window of the data recorded on 19 Decem-
 254 ber 2016. The dominance of static clutter is very evident in the unprocessed data, and
 255 it is somewhat remarkable that a relatively simple clutter-suppression algorithm is so suc-



271 **Figure 4.** Representative 2 hr period of radar data acquired on 19 December 2016 showing
 272 raw slant-range data (top), slant-range data following clutter suppression (middle), lake level
 273 relative to its mean (bottom). Green crosses show the lake level measurements and the blue line
 274 shows the median filtered data (kernel size of 13).

256 cessful at removing it and revealing the variations in lake height so clearly. Lake level
 257 is plotted as a relative height about its mean value, showing variations on the order of
 258 ± 0.5 m. This is consistent with the lake level changes measured by *Jones et al.* [2015]
 259 using TLS in 2010. The fluctuations in lake level shown in Fig. 4 exhibit a cyclic behaviour
 260 with a period of ~ 15 min. This is a well-recognised behaviour of the Erebus lake as noted
 261 by numerous previous studies [*Oppenheimer et al.*, 2009; *Peters et al.*, 2014a,b; *Ilanko*
 262 *et al.*, 2015].

263 The lake levels presented in Fig. 4 show a random measurement to measurement
 264 deviation of ± 0.5 m. We attribute this scatter to uncertainties in the Gaussian fitting,
 265 and the rapidly changing specular nature of the lake surface itself. Some measurements
 266 (e.g. at 16:14:20 UTC) show deviations of a few metres from their neighbouring mea-
 267 surements. These are caused by metre-scale bubbles bursting at the lake’s surface, form-
 268 ing a strong radar target at a particular range and skewing the Gaussian fit towards that
 269 range. This is confirmed by inspection of coincident thermal imagery collected with an
 270 automated infrared camera system [*Peters et al.*, 2014c].

275 6 Conclusions

276 We have presented the Eredar instrument, a new FMCW radar system designed
 277 for monitoring the level of active lava lakes, which was successfully deployed on Erebus

278 volcano, Antarctica in December 2016. The dataset recorded during this deployment is
 279 the longest continuous measure of lake level at Erebus to date and clearly demonstrates
 280 the potential of radar instruments for prolonged and continuous surveillance of lava lake
 281 level.

282 Future refinement of the system will include reducing power consumption, increas-
 283 ing acquisition rate and incorporating on-board data processing capabilities. The envis-
 284 aged endpoint is a system suitable for long-term operational monitoring in support of
 285 volcanological research and hazard assessment.

286 Acknowledgments

287 This work was supported by the Isaac Newton Trust project "Physical constraints for
 288 the interpretation of open-vent volcanism" and NERC [grant NE/N009312/1]. CO is ad-
 289 ditionally supported by the NERC Centre for the Observation and Modelling of Volca-
 290 noes, Earthquakes and Tectonics (COMET). Field support was provided by the NSF un-
 291 der award ANT1142083. NP wishes to thank Aaron Curtis and Tim & Zoe Burton for
 292 their help during fieldwork. The radar data presented in this article may be obtained
 293 from <https://doi.org/10.6084/m9.figshare.6480275.v1>.

294 References

- 295 Ash, M., and P. V. Brennan (2015), Transmitter noise considerations in super-
 296 Nyquist FMCW radar design, *Electronics Letters*, 51(5), 413–415, doi:
 297 10.1049/el.2014.4236.
- 298 Ash, M., M. A. Tanha, P. V. Brennan, A. Köhler, J. N. McElwaine, and C. J. Key-
 299 lock (2014), Improving the sensitivity and phased array response of FMCW radar
 300 for imaging avalanches, in *2014 International Radar Conference*, pp. 1–5, doi:
 301 10.1109/RADAR.2014.7060387.
- 302 Ash, M., M. Ritchie, and K. Chetty (2018), On the Application of Digital Moving
 303 Target Indication Techniques to Short-Range FMCW Radar Data, *IEEE Sensors*
 304 *Journal*, 18(10), 4167–4175, doi:10.1109/JSEN.2018.2823588.
- 305 Brennan, P. V., L. B. Lok, K. Nicholls, and H. Corr (2014), Phase-sensitive FMCW
 306 radar system for high-precision Antarctic ice shelf profile monitoring, *IET Radar,*
 307 *Sonar & Navigation*, 8(7), 776–786, doi:10.1049/iet-rsn.2013.0053.
- 308 Dibble, R., P. Kyle, and C. Rowe (2008), Video and seismic observations of Strom-
 309 bolian eruptions at Erebus volcano, Antarctica, *Journal of Volcanology and*
 310 *Geothermal Research*, 177(3), 619–634, doi:10.1016/j.jvolgeores.2008.07.020.
- 311 Gerst, A., M. Hort, R. C. Aster, J. B. Johnson, and P. R. Kyle (2013), The first
 312 second of volcanic eruptions from the Erebus volcano lava lake, Antarctica - ener-
 313 gies, pressures, seismology, and infrasound, *Journal of Geophysical Research: Solid*
 314 *Earth*, 118(7), 3318–3340, doi:10.1002/jgrb.50234.
- 315 Giggenbach, W. F., P. R. Kyle, and G. L. Lyon (1973), Present volcanic activity on
 316 Mount Erebus, Ross Island, Antarctica, *Geology*, 1(3), 135–136.
- 317 Griffiths, H. D. (1990), New ideas in FM radar, *Electronics Communication Engi-*
 318 *neering Journal*, 2(5), 185–194, doi:10.1049/ecej:19900043.
- 319 Hyun, E., Y.-S. Jin, and J.-H. Lee (2016), A Pedestrian Detection Scheme Using a
 320 Coherent Phase Difference Method Based on 2D Range-Doppler FMCW Radar,
 321 *Sensors*, 16(1), 124, doi:10.3390/s16010124.
- 322 Ilanko, T., C. Oppenheimer, A. Burgisser, and P. Kyle (2015), Cyclic de-
 323 gassing of Erebus volcano, Antarctica, *Bulletin of Volcanology*, 77(6), 56, doi:
 324 10.1007/s00445-015-0941-z.
- 325 Jones, K. R., J. B. Johnson, R. Aster, P. R. Kyle, and W. McIntosh (2008), In-
 326 frasonic tracking of large bubble bursts and ash venting at Erebus volcano,
 327 Antarctica, *Journal of Volcanology and Geothermal Research*, 177(3), 661–672,

- 328 doi:10.1016/j.jvolgeores.2008.02.001.
- 329 Jones, L. K., P. R. Kyle, C. Oppenheimer, J. D. Frechette, and M. H. Okal (2015),
 330 Terrestrial laser scanning observations of geomorphic changes and varying lava
 331 lake levels at Erebus volcano, Antarctica, *Journal of Volcanology and Geothermal
 332 Research*, 295, 43–54, doi:10.1016/j.jvolgeores.2015.02.011.
- 333 Kelly, P. J., P. R. Kyle, N. W. Dunbar, and K. W. Sims (2008), Geochemistry and
 334 mineralogy of the phonolite lava lake, Erebus volcano, Antarctica: 1972-2004 and
 335 comparison with older lavas, *Journal of Volcanology and Geothermal Research*,
 336 177(3), 589–605, doi:10.1016/j.jvolgeores.2007.11.025.
- 337 Lok, L. B., P. V. Brennan, M. Ash, and K. W. Nicholls (2015), Autonomous phase-
 338 sensitive radio echo sounder for monitoring and imaging antarctic ice shelves,
 339 in *2015 8th International Workshop on Advanced Ground Penetrating Radar
 340 (IWAGPR)*, pp. 1–4, doi:10.1109/IWAGPR.2015.7292636.
- 341 Marshall, H.-P., and G. Koh (2008), FMCW radars for snow research, *Cold Regions
 342 Science and Technology*, 52(2), 118–131, doi:10.1016/j.coldregions.2007.04.008.
- 343 Martone, A. F., K. Ranney, and C. Le (2014), Noncoherent Approach for Through-
 344 the-Wall Moving Target Indication, *IEEE Transactions on Aerospace and Elec-
 345 tronic Systems*, 50(1), 193–206, doi:10.1109/TAES.2013.120329.
- 346 Oppenheimer, C., A. S. Lomakina, P. R. Kyle, N. G. Kingsbury, and M. Boichu
 347 (2009), Pulsatory magma supply to a phonolite lava lake, *Earth and Planetary
 348 Science Letters*, 284(3-4), 392–398, doi:10.1016/j.epsl.2009.04.043.
- 349 Orr, T. R., and J. C. Rea (2012), Time-lapse camera observations of gas piston ac-
 350 tivity at Pu’u ’Ō’ō, Kīlauea volcano, Hawai’i, *Bulletin of Volcanology*, 74(10),
 351 2353–2362, doi:10.1007/s00445-012-0667-0.
- 352 Patrick, M. R., T. Orr, L. Antolik, L. Lee, and K. Kamibayashi (2014), Continu-
 353 ous monitoring of Hawaiian volcanoes with thermal cameras, *Journal of Applied
 354 Volcanology*, 3(1), 1, doi:10.1186/2191-5040-3-1.
- 355 Patrick, M. R., T. Orr, D. A. Swanson, and E. Lev (2016), Shallow and deep con-
 356 trols on lava lake surface motion at Kīlauea Volcano, *Journal of Volcanology and
 357 Geothermal Research*, 328, 247–261, doi:10.1016/j.jvolgeores.2016.11.010.
- 358 Peters, N., C. Oppenheimer, D. R. Killingsworth, J. Frechette, and P. Kyle (2014a),
 359 Correlation of cycles in Lava Lake motion and degassing at Erebus Volcano,
 360 Antarctica, *Geochemistry, Geophysics, Geosystems*, 15(8), 3244–3257, doi:
 361 10.1002/2014GC005399.
- 362 Peters, N., C. Oppenheimer, P. Kyle, and N. Kingsbury (2014b), Decadal persistence
 363 of cycles in lava lake motion at Erebus volcano, Antarctica, *Earth and Planetary
 364 Science Letters*, 395, 1–12, doi:10.1016/j.epsl.2014.03.032.
- 365 Peters, N., C. Oppenheimer, and P. Kyle (2014c), Autonomous thermal cam-
 366 era system for monitoring the active lava lake at Erebus volcano, Antarctica,
 367 *Geoscientific Instrumentation, Methods and Data Systems*, 3(1), 13–20, doi:
 368 10.5194/gi-3-13-2014.
- 369 Rose, W. I., J. L. Palma, H. D. Granados, and N. Varley (2013), Understanding
 370 Open-Vent Volcanism and Related Hazards, Geological Society of America.
- 371 Smets, B., N. d’Oreye, M. Kervyn, and F. Kervyn (2017), Gas piston activ-
 372 ity of the Nyiragongo lava lake: First insights from a Stereographic Time-
 373 Lapse Camera system, *Journal of African Earth Sciences*, 134, 874–887, doi:
 374 10.1016/j.jafrearsci.2016.04.010.
- 375 Stove, A. G. (1992), Linear FMCW radar techniques, *IEE Proceedings F - Radar
 376 and Signal Processing*, 139(5), 343–350, doi:10.1049/ip-f-2.1992.0048.
- 377 Stove, A. G. (2004), Modern FMCW radar - techniques and applications, in *First
 378 European Radar Conference, 2004. EURAD.*, pp. 149–152.
- 379 Tazieff, H. (1994), Permanent lava lakes: observed facts and induced mecha-
 380 nisms, *Journal of Volcanology and Geothermal Research*, 63(1-2), 3–11, doi:
 381 10.1016/0377-0273(94)90015-9.

382 Telling, J., A. Lyda, P. Hartzell, and C. Glennie (2017), Review of Earth science
383 research using terrestrial laser scanning, *Earth-Science Reviews*, *169*, 35–68, doi:
384 10.1016/j.earscirev.2017.04.007.